

Received 21 May 2019; revised 31 May 2019; accepted 1 June 2019. Date of publication 5 June 2019; date of current version 27 June 2019.
 The review of this paper was arranged by Editor M. Chan.

Digital Object Identifier 10.1109/JEDS.2019.2920856

Incorporating Resistance Into the Transition From Field Emission to Space Charge Limited Emission With Collisions

SAMUEL D. DYNAKO¹, ADAM M. DARR² (Student Member, IEEE),
 AND ALLEN L. GARNER^{1,2} (Senior Member, IEEE)

¹ School of Electrical and Computer Engineering, Purdue University, West Lafayette, IN 47907, USA

² School of Nuclear Engineering, Purdue University, West Lafayette, IN 47907, USA

CORRESPONDING AUTHOR: A. L. GARNER (e-mail: algarner@purdue.edu)

This work was supported in part by the Air Force Office of Scientific Research under Award FA9550-18-1-0218, in part by the Purdue Doctoral Fellowship, and in part by the Purdue Summer University Research Fellowship.

ABSTRACT Field emitters and microplasmas often use series resistors to mitigate the rapid increase in current density that reduces device stability. This paper investigates the impact of external resistance on the transition of electron emission mechanism as a function of applied voltage V_{app} , gap distance D , and electron mobility μ . For low μ (high gas pressure), the circuit transitions from Fowler–Nordheim (FN) to space charge limited emission by Mott–Gurney (MG) and Child–Langmuir (CL) before reaching Ohm’s law (OL). At higher μ , a triple point arises where the asymptotic solutions for FN, MG, and CL intersect. This triple point is uniquely defined by D , μ , or gap voltage V_g while also defining a specific gap impedance Z_{tp} . When $R \leq Z_{tp}$, the electron emission transitions from FN to MG to CL to OL with increasing V_{app} while MG and CL are bypassed at higher R . For a given R , increasing the applied voltage or emission current causes the gap to appear as a short.

INDEX TERMS Electron emission, plasma devices, space-charge effect.

I. INTRODUCTION

Electron emission is an important phenomenon in high brightness electron sources [1]–[2], light sources [3], vacuum electronics [4]–[5], and microdischarges [6] where one desires to avoid gas breakdown for microdevices and induce gas breakdown for microplasmas. Numerous studies have examined the phenomena behind electron emission [4]–[5], [7]–[13], particularly the transition from field emission, given by the Fowler–Nordheim (FN) equation, to space charge limited emission (SCLE) given by the Child–Langmuir (CL) law at vacuum [7]–[12] and Mott–Gurney (MG) law at general pressure [13]. Asymptotic studies have predicted the transition from FN to CL at vacuum [7], CL to MG for plasma sheaths [13], and FN to Paschen’s law for microscale gas breakdown [14]–[17]. We have recently derived asymptotic relationships to determine the transition between CL, FN, and MG by incorporating frictional loss into the electron motion equation, as well as demonstrating the existence of a “triple point”

where all three asymptotic solutions match [18]. The “triple point” provides practical design insight by giving the critical mobility/pressure under which electron emission will transition directly from FN to CL, while bypassing the MG regime [18], which has important implications when predicting gas breakdown for sub-microscale gaps to indicate the appropriate SCLE mechanism that drives the transition [16].

Because electron emission current density increases rapidly with voltage, which is deleterious to emitter stability, one may add a series resistor to improve stability [19]; however, this may increase operating voltage and cost while reducing efficiency [20]. Similarly, one may add an external resistor to control device current in microplasma devices [21]–[23]. These experiments [21] motivated one-dimensional planar particle-in-cell (PIC) simulations incorporating an external resistor [22] with good agreement with experimental results [21]; however, the conditions were not in the field emission dominated regime.

These studies indicate the importance of characterizing the transition between electron emission and breakdown regimes with external lumped circuit elements, such as external resistors, which play pivotal roles in controlling system current and may also change the dominant emission and breakdown regime. While a theoretical study explored this behavior by extending the asymptotic theory unifying CL and FN [7] with an external resistor [20] in vacuum, applying this behavior to microplasmas or even to vacuum devices with slight leakage requires incorporating collisions. Analogous to [20], which elucidated the regimes where field emission and the resistor dominate, the current study extends our previous work incorporating collisions into the transition from FN to SCLE [18] by adding a series resistor. This permits the simultaneous exploration of the impact of collisions and an external resistor on the transition between CL, MG, and FN. For a sufficiently large resistance, the gap has *negligible* effects on the circuit, which is critical for many experimental setups [21]. This analysis has important practical implications on selecting a sufficient resistance to effectively minimize current without necessitating an impractically high applied voltage.

II. MODELING AND ANALYSIS

Similar to our previous study to assess the impact of collisions on the transition from field emission to space-charge limited emission [18], we consider a one-dimensional, planar geometry with the parallel plates separated by gap distance D , gap voltage V_g , and a neutral gas with electron mobility μ , giving a diode impedance Z as a function of V_g and current density J . In this case, we include a resistor of resistance R in series with diode and the applied voltage V_{app} , such that $V_{app} \neq V_g$. The resulting circuit equation is

$$V_{app} = V_g + IR = I(Z + R), \quad (1)$$

with $Z \equiv V_g/(JS)$ and current $I \equiv JS$ for emitter surface area S .

To reduce parameters, we nondimensionalize by defining

$$\begin{aligned} \phi &= \phi_0 \bar{\phi}; J = J_0 \bar{J}; x = x_0 \bar{x}; t = t_0 \bar{t}; \mu = \mu_0 \bar{\mu}; \\ E &= E_0 \bar{E}; v = v_0 \bar{v}; Z = Z_0 \bar{Z}; R = Z_0 \bar{R}, \end{aligned} \quad (2)$$

where ϕ is the electric potential, x is the spatial coordinate, t is time, E is electric field, and v is the electron velocity. The bars denote dimensionless parameters and the terms with subscript 0 represent the scaling terms, given by

$$\begin{aligned} \phi_0 &= \frac{e\epsilon_0^2}{mA^2}; J_0 = AB^2; x_0 = \frac{e\epsilon_0^2}{mA^2B}; t_0 = \frac{\epsilon_0}{AB}; \\ \mu_0 &= \frac{e\epsilon_0}{mAB}; E_0 = B; v_0 \equiv \frac{x_0}{t_0}; Z_0 = \frac{\phi_0}{J_0 S}, \end{aligned} \quad (3)$$

where e is the electron charge, ϵ_0 is the permittivity of free space, A and B are FN coefficients, and m is the electron mass. We calculate \bar{V}_g and \bar{J} as in [18].

Asymptotically, we observe transitions in electron emission mechanism without a resistor [18] if we consider only \bar{V}_g . Specifically, we obtain the FN solution given by

$$\bar{J}_{FN} = \bar{E}^2 \exp(-1/\bar{E}), \quad (4)$$

where $\bar{E} = \bar{V}_g/\bar{D}$ in the absence of space charge when $\bar{\mu}^{-1} \geq 9 \exp(\bar{D}/\bar{V}_g)/(8\bar{D})$; the CL limit of

$$\bar{J}_{CL} = 4\sqrt{2}\bar{V}_g^{3/2}/(9\bar{D}^2), \quad (5)$$

when $81\bar{V}_g^{1/2}/(32\bar{D}\sqrt{2}) \leq \bar{\mu}^{-1} \leq 9 \exp(\bar{D}/\bar{V}_g)/(8\bar{D})$; and the MG limit of

$$\bar{J}_{MG} = 9\bar{\mu}\bar{V}_g^2/(8\bar{D}^3), \quad (6)$$

when $\bar{\mu}^{-1} \leq 81\bar{V}_g^{1/2}/(32\bar{D}\sqrt{2})$. For $\bar{R} = 0$, in (4)-(6) $\bar{V}_g \equiv \bar{V}_{app}$. When $\bar{R} \gg \bar{Z}$ in (1), the entire circuit will tend toward Ohm's law (OL), or

$$\bar{J}_{Ohm} = \bar{V}_{app}/\bar{R}. \quad (7)$$

Figure 1a shows the transitions between the asymptotic solutions in (4)-(7) for $\bar{D} = 10^7$, $\bar{\mu} = 0.7$, and $\bar{R} = 10^4$ as a function of \bar{V}_{app} . The solution follows the minimum energy or minimum current principle, following the asymptotic relation giving the lowest \bar{V}_{app} at a particular \bar{J} , with modified behavior at transitions between asymptotes. At low \bar{J} and \bar{V}_{app} , the effect of the resistor is vanishingly small upon the circuit; the opposite holds at high \bar{J} and \bar{V}_{app} when the gap becomes negligible. As before [18], gap emission behavior transitions from FN to MG to CL as \bar{V}_{app} increases; however, the external resistor causes the overall circuit to exhibit predominantly OL at very high \bar{J} and \bar{V}_{app} . While real devices operate in a much narrower range of \bar{J} and \bar{V} than depicted in Fig. 1a, Fig. 1a demonstrates the conditions for transitioning between or operating within any combination of emission conditions.

Figure 1b assesses the transitions with varying \bar{R} at constant $\bar{\mu} = 4843$ and $\bar{D} = 10^7$ to match triple point conditions [18]. The dimensionless impedance at the triple point is $\bar{Z}_{tp} = 1.38 \times 10^{11}$. To assess the influence of an external resistor, we consider $\bar{R} = \bar{Z}_{tp}$, $\bar{R} \ll \bar{Z}_{tp}$, and $\bar{R} \gg \bar{Z}_{tp}$. For $\bar{R} > \bar{Z}_{tp}$, the behavior transitions directly from FN to OL. At $\bar{R} = \bar{Z}_{tp}$ the FN, CL, and MG asymptotes intersect with OL, again resulting in the direct transition from FN to OL. When $0 < \bar{R} < \bar{Z}_{tp}$, emission transitions from FN to CL (since it passes through the triple point) to Ohm's law with the space-charge regime controllable by altering the resistance.

These transitions occur gradually. Figure 2a shows the quotient between the voltage predicted in (4)-(7) and \bar{V}_{app} as a function of \bar{J} ; for (4)-(6), we assume $\bar{R} = 0$, asymptotically. While each regime (FN, MG, CL, OL) has a region where it dominates ($\bar{V}_{g0}/\bar{V}_{app} \approx 1$, where \bar{V}_{g0} represents one of the limits from (4)-(6)), there are also large, transitional regions. During these transitions, the fractions do not add to unity because there is no clear demarcation between regimes, nor are they independent of each other. Thus, despite the

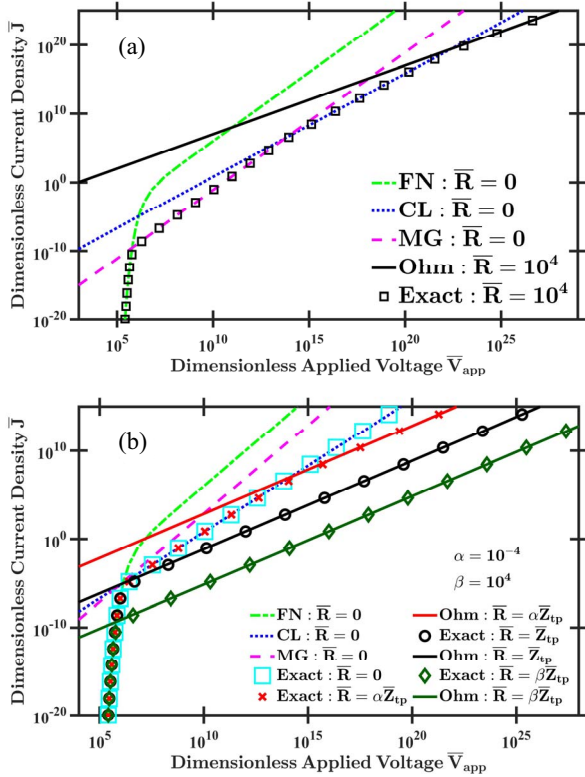


FIGURE 1. Exact and asymptotic solution for dimensionless current density \bar{J} as a function of dimensionless applied voltage \bar{V}_{app} for dimensionless gap distance $\bar{D} = 10^7$. (a) For dimensionless electron mobility $\bar{\mu} = 0.4843$, electron emission transitions from Fowler-Nordheim (FN) to Mott-Gurney (MG) to Child-Langmuir (CL) for increasing \bar{V}_{app} for dimensionless resistance $\bar{R} = 0$. For $\bar{R} = 10^4$, \bar{J} eventually follows Ohm's Law (OL). (b) For $\bar{\mu} = 4843$, the asymptotic solutions for FN, MG, and CL intersect at the triple point for $\bar{R} = 0$. Electron emission transitions from FN to CL for increasing \bar{V}_{app} for $\bar{R} \leq \bar{Z}_{tp} = 1.38 \times 10^{11}$, where \bar{Z}_{tp} is the gap impedance at the triple point. When $0 \leq \bar{R} \leq \bar{Z}_{tp}$, electron emission transitions from FN to CL to OL. When $\bar{R} > \bar{Z}_{tp}$, electron emission transitions directly from FN to OL.

asymptotic limits intersecting abruptly, a gap operating in these intermediate regimes cannot be fully modeled by a single scaling law, even several orders of magnitude away from the transition point between any/all of (4)-(7).

Figure 2b shows that at the triple point, where the four asymptotic solutions intersect (including $\bar{R} = \bar{Z}_{tp}$), (4)-(7) are less than 40% accurate. In this case, the full solution for \bar{V}_g and \bar{J} from [18] must be coupled with (1) to obtain accurate results.

Practically, the resistor acts as a voltage divider. At the intersection of OL for $\bar{R} = \bar{Z}_{tp}$ and the exact solution for $\bar{R} = 0$, voltage is divided evenly between the circuit elements. The voltage division effect is spread over several orders of magnitude for \bar{V}_{app} and \bar{J} and varies linearly on a semi-log scale when $\bar{R} \approx \bar{Z}_g$. In addition, for low \bar{V}_{app} and \bar{J} , $\bar{V}_{app} \approx \bar{V}_g$. These conditions facilitate conversion between \bar{V}_{app} and \bar{V}_g . Thus, the specific electron emission mechanism may be tunable by appropriate selection of applied voltage, injected current, or external resistor.

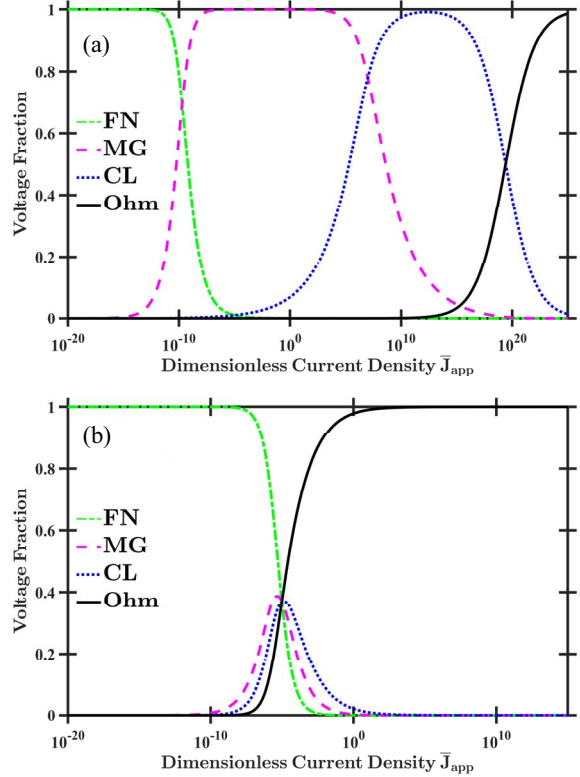


FIGURE 2. Fraction of actual applied voltage \bar{V}_{app} to \bar{V}_g predicted by (4)-(6) for $\bar{R} = 0$ and \bar{V}_{app} predicted by (7) as a function of dimensionless current density \bar{J}_{app} (a) for dimensionless gap distance $\bar{D} = 10^7$, dimensionless electron mobility $\bar{\mu} = 0.4843$, and dimensionless resistance $\bar{R} = 10^4$ and (b) for $\bar{D} = 10^7$, $\bar{\mu} = 4843$ (the triple point $\bar{\mu}$ for this \bar{D}), and $\bar{R} = \bar{Z}_{tp}$ where \bar{Z}_{tp} is the triple point impedance for this $\bar{\mu}$. These fractions do not necessarily sum to unity. (b) Voltage fraction for a triple point condition, where the Fowler-Nordheim (FN) relation, Mott-Gurney (MG) law, and Child-Langmuir (CL) law intersect.

Figure 3 shows the impact of moderate \bar{J} and \bar{V}_{app} on the division of voltage across the gap and resistor. At low \bar{J} , the resistor is negligible and most of the voltage is across the gap, causing the behavior to more closely mimic $\bar{R} = 0$ in the FN regime. As \bar{J} increases, the voltage across the gap and resistor match, corresponding to the triple point. At higher \bar{J} , Fig. 1 shows that OL dominates, as indicated in Fig. 3 by the resistor having a higher potential difference than the gap.

Figure 4 shows the unique conditions of $\bar{\mu}_{tp}$, \bar{D}_{tp} , and $\bar{V}_{g, tp}$ that yield the triple point [18] with the corresponding \bar{Z}_{tp} . Selecting any of the first three parameters uniquely defines the other three for the triple point. Fig. 1b shows that selecting $\bar{R} \leq \bar{Z}_{tp}$ ensures that electron emission will transition from FN to CL to OL with increasing \bar{V}_g or \bar{J} .

As a practical example, we apply (2) and (3) with $A = (1.4/\varphi) \times 10^{-6+4.26/\sqrt{\varphi}}$ and $B = 6.49 \times 10^9 \varphi^{1.5}$ [18], for $\varphi = 4$ eV, $\phi_0 = 6.18 \times 10^{-3}$ V, $x_0 = 1.19 \times 10^{-13}$ m, $J_0 = 1.27 \times 10^{17}$ A/m², $\mu_0 = 6.35 \times 10^{-7}$ m²/(Vs), and $Z_0 = 1.21 \times 10^{-4}$ Ω. Choosing gap distance $D = 250$ nm ($\bar{D} = 2.1 \times 10^6$) and emission area $S = 4 \times 10^{-16}$ m²

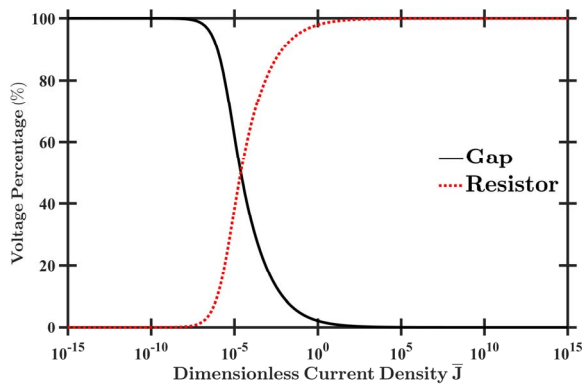


FIGURE 3. Fraction of applied dimensionless voltage \bar{V}_{app} across the diode and resistor as a function of dimensionless current density \bar{J} for dimensionless gap distance $\bar{D} = 10^7$, dimensionless resistance $R = \bar{Z} = 1.38 \times 10^{11}$ – the dimensionless impedance at the triple point – and dimensionless electron mobility $\bar{\mu} = 7000$. For low \bar{J} , the resistor is negligible, while the gap acts as a short at high \bar{J} . The resistor matches the gap impedance at the triple point.

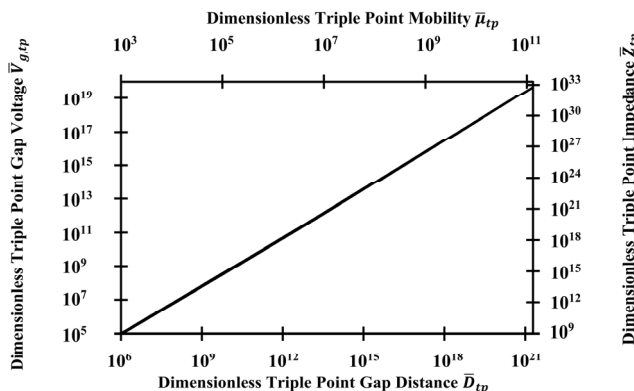


FIGURE 4. Dimensionless gap voltage $\bar{V}_{g, tp}$, distance \bar{D}_{tp} , mobility $\bar{\mu}_{tp}$, and gap impedance \bar{Z}_{tp} at the triple point, where the asymptotic solutions for Fowler-Nordheim, Mott-Gurney, and Child-Langmuir intersect. Adding an external resistor R that matches \bar{Z}_{tp} causes Ohm's law to intersect at the triple point and the resistor to act as a triple-point voltage divider.

(side length of 20 nm to avoid edge effects from finite diode), $\bar{V}_g = 3.09 \times 10^5$ ($V_g = 1.91$ kV), $\bar{\mu} = 2.11 \times 10^3$ ($\mu = 1.34 \times 10^{-3}$ m²/(Vs)), and vacuum surface field $E = V_g/D = 7.65 \times 10^9$ V/m since we can approach the triple point from FN. At the triple point, $J = 3.12 \times 10^{12}$ A/m² and $I = 1.25$ mA. Defining $v_d \equiv \mu E$ gives the electron drift velocity for this system as $v_d = 1.02 \times 10^7$ m/s. For nitrogen, $v_e = 3.3 \times 10^6 (E/P)^{1/2}$ where v_e and E are in cgs units and P is in Torr [24], giving $P = 794$ Torr. This suggests that the gap acts like vacuum at any pressure below one atmosphere for these conditions. While the triple point is not directly related to the mean-free path, this gap distance is on the order of the mean-free path in air, which we recently estimated as 539 nm at 760 Torr [25]. Finally, $\bar{Z}_{tp} = 1.26 \times 10^{10}$ ($Z_{tp} = 1.53$ MΩ); thus, selecting $R > 1.53$ MΩ would mask any SCLE (CL or MG) behavior in the I-V characteristics

of the circuit, regardless of pressure. However, applying sufficient E to achieve the triple point in this condition may cause cathode breakdown before satisfying the triple point condition. This shows the value of the triple point as a diagnostic; an experimentalist can surmise, knowing only D and p , that this example gap will normally operate purely in the FN mode for $V < 1.91$ kV. The triple point also predicts the conditions necessary for the existence of the MG regime; above the triple point pressure, emission will transition from FN to MG to CL, while lower pressures exhibit vacuum-like behavior over the entire spectrum of V and J . Furthermore, tuning the external resistor may allow modifying the potential difference across the gap to control electron emission behavior.

III. CONCLUSION

This paper demonstrates the impact of the transition of electron emission mechanism from adding a resistor in series with a diode and voltage source. The gap behavior transitions from FN to MG to CL; the resistor causes the circuit to transition to OL when $R \gg Z_g$. The triple point where FN, MG, and CL intersect is defined by selecting V_g , μ (or pressure), or D , which uniquely defines the other two parameters and the gap impedance, Z_{tp} . When $R < Z_{tp}$, electron emission transitions from FN to CL directly, while electron emission transitions from FN to OL when $R > Z_{tp}$. Thus, the resistance plays a critical role in the significance of space charge on emission, which has important effects on field emitters in both vacuum [20] and microplasma generation [22]. This becomes particularly important as gap size is reduced below ~ 1 μm [17], which is close to the triple point for nitrogen [18], which should be close to that of air. This motivates additional consideration of resistor selection in circuit design for driving microplasmas or assuring reliability when designing microscale or nanoscale electronics.

REFERENCES

- [1] F. Houdellier *et al.*, “Development of TEM and SEM high brightness electron guns using cold-field emission from a carbon nanotip,” *Ultramicroscopy*, vol. 151, pp. 107–115, Apr. 2015. doi: [10.1016/j.ultramic.2014.11.021](https://doi.org/10.1016/j.ultramic.2014.11.021).
- [2] W. B. Choi *et al.*, “Fully sealed, high-brightness carbon-nanotube field-emission display,” *Appl. Phys. Lett.*, vol. 75, no. 20, pp. 3129–3131, 1999. doi: [10.1063/1.125253](https://doi.org/10.1063/1.125253).
- [3] F. Pyatkov *et al.*, “Cavity-enhanced light emission from electrically driven carbon nanotubes,” *Nat. Photon.*, vol. 10, pp. 420–427, Apr. 2016. doi: [10.1038/nphoton.2016.70](https://doi.org/10.1038/nphoton.2016.70).
- [4] P. Zhang, A. Vafells, L. K. Ang, J. W. Luginsland, and Y. Y. Lau, “100 years of the physics of diodes,” *Appl. Phys. Rev.*, vol. 4, no. 1, 2017, Art. no. 011304. doi: [10.1063/1.4978231](https://doi.org/10.1063/1.4978231).
- [5] K. L. Jensen, “A tutorial on electron sources,” *IEEE Trans. Plasma Sci.*, vol. 46, no. 6, pp. 1881–1889, Jun. 2018. doi: [10.1109/TPS.2017.2782485](https://doi.org/10.1109/TPS.2017.2782485).
- [6] D. B. Go and A. Venkatraman, “Microscale gas breakdown: Ion-enhanced field emission and the modified Paschen’s curve,” *J. Phys. D Appl. Phys.*, vol. 47, no. 50, 2014, Art. no. 503001. doi: [10.1088/0022-3727/47/50/503001](https://doi.org/10.1088/0022-3727/47/50/503001).
- [7] Y. Y. Lau, Y. Liu, and R. K. Parker, “Electron emission: From the Fowler-Nordheim relation to the Child-Langmuir law,” *Phys. Plasmas*, vol. 1, no. 6, pp. 2082–2085, 1994. doi: [10.1063/1.870603](https://doi.org/10.1063/1.870603).
- [8] Y. Feng and J. Verboncoeur, “Transition from Fowler-Nordheim field emission to space charge limited current density,” *Phys. Plasmas*, vol. 13, no. 7, 2006, Art. no. 073105. doi: [10.1063/1.2226977](https://doi.org/10.1063/1.2226977).

- [9] R. G. Forbes, "Exact analysis of surface field reduction due to field-emitted vacuum space charge, in parallel-plane geometry, using simple dimensionless equations," *J. Appl. Phys.*, vol. 104, no. 8, 2008, Art. no. 084303. doi: [10.1063/1.2996005](https://doi.org/10.1063/1.2996005).
- [10] A. Rokhlenko, K. L. Jensen, and J. L. Lebowitz, "Space charge effects in field emission: One dimensional theory," *J. Appl. Phys.*, vol. 107, no. 1, 2010, Art. no. 014904. doi: [10.1063/1.3272690](https://doi.org/10.1063/1.3272690).
- [11] K. L. Jensen, J. Lebowitz, Y. Y. Lau, and J. Luginsland, "Space charge and quantum effects on electron emission," *J. Appl. Phys.*, vol. 111, no. 5, 2012, Art. no. 054917. doi: [10.1063/1.3692577](https://doi.org/10.1063/1.3692577).
- [12] K. L. Jensen *et al.*, "Discrete space charge affected field emission: Flat and hemisphere emitters," *J. Appl. Phys.*, vol. 117, no. 19, 2015, Art. no. 194902. doi: [10.1063/1.4921186](https://doi.org/10.1063/1.4921186).
- [13] M. S. Benilov, "The Child-Langmuir law and analytical theory of collisionless to collision-dominated sheaths," *Plasma Sources Sci. Technol.*, vol. 18, no. 1, 2008, Art. no. 014005. doi: [10.1088/0963-0252/18/1/014005](https://doi.org/10.1088/0963-0252/18/1/014005).
- [14] A. M. Loveless and A. L. Garner, "Scaling laws for gas breakdown for nanoscale to microscale gaps at atmospheric pressure," *Appl. Phys. Lett.*, vol. 108, no. 23, 2016, Art. no. 234103. doi: [10.1063/1.4953202](https://doi.org/10.1063/1.4953202).
- [15] A. M. Loveless and A. L. Garner, "Generalization of microdischarge scaling laws for all gases at atmospheric pressure," *IEEE Trans. Plasma Sci.*, vol. 45, no. 4, pp. 574–583, Apr. 2017. doi: [10.1109/TPS.2017.2647988](https://doi.org/10.1109/TPS.2017.2647988).
- [16] A. M. Loveless and A. L. Garner, "A universal theory for gas breakdown from microscale to the classical Paschen law," *Phys. Plasmas*, vol. 24, no. 11, 2017, Art. no. 113522. doi: [10.1063/1.5004654](https://doi.org/10.1063/1.5004654).
- [17] G. Meng *et al.*, "Demonstration of field emission driven microscale gas breakdown for pulsed voltages using *in-situ* optical imaging," *Phys. Plasmas*, vol. 25, no. 8, 2018, Art. no. 082116. doi: [10.1063/1.5046335](https://doi.org/10.1063/1.5046335).
- [18] A. M. Darr, A. M. Loveless, and A. L. Garner, "Unification of field emission and space charge limited emission with collisions," *Appl. Phys. Lett.*, vol. 114, no. 1, 2019, Art. no. 014103. doi: [10.1063/1.5066236](https://doi.org/10.1063/1.5066236).
- [19] J. D. Levine, R. Meyer, R. Baptist, T. E. Felter, and A. A. Talin, "Field emission from microtip test arrays using resistor stabilization," *J. Vac. Sci. Technol. B Microelectron. Nanometer Struct. Process. Meas. Phenom.*, vol. 13, no. 2, pp. 474–477, 1995. doi: [10.1116/1.588336](https://doi.org/10.1116/1.588336).
- [20] J. W. Luginsland, A. Valfells, and Y. Y. Lau, "Effects of a series resistor on electron emission from a field emitter," *Appl. Phys. Lett.*, vol. 69, no. 18, pp. 2770–2772, 1996. doi: [10.1063/1.117670](https://doi.org/10.1063/1.117670).
- [21] S. Kunuku, K. J. Sankaran, C.-L. Dong, N.-H. Tai, K.-C. Leou, and I.-N. Lin, "Development of long lifetime cathode materials for microplasma application," *RSC Adv.*, vol. 4, no. 88, pp. 47865–47875, 2014. doi: [10.1039/C4RA08296F](https://doi.org/10.1039/C4RA08296F).
- [22] A. Venkatraman, "Theory and analysis of operating modes in microplasmas assisted by field emitting cathodes," *Phys. Plasmas*, vol. 22, no. 5, 2015, Art. no. 057102. doi: [10.1063/1.4921335](https://doi.org/10.1063/1.4921335).
- [23] M. A. Bilici, J. R. Haase, C. R. Boyle, D. B. Go, and R. M. Sankaran, "The smooth transition from field emission to a self-sustained plasma in microscale electrode gaps at atmospheric pressure," *J. Appl. Phys.*, vol. 119, no. 22, 2016, Art. no. 22301. doi: [10.1063/1.4953648](https://doi.org/10.1063/1.4953648).
- [24] N. M. Zubarev and S. N. Ivanov, "Mechanism of runaway electron generation at gas pressures from a few atmospheres to several tens of atmospheres," *Plasma Phys. Rep.*, vol. 44, no. 4, pp. 445–452, 2018. doi: [10.1134/S1063780X18040104](https://doi.org/10.1134/S1063780X18040104).
- [25] G. Meng *et al.*, "Spatio-temporal dynamics of pulsed gas breakdown in microgaps," *Phys. Plasmas*, vol. 26, no. 1, 2019, Art. no. 014506. doi: [10.1063/1.5081009](https://doi.org/10.1063/1.5081009).



SAMUEL D. DYNAKO is currently pursuing the B.S. degree in electrical and computer engineering with Purdue University, West Lafayette, IN, USA, where he was with the Bioelectronics and Electrophysics Laboratory for almost two years. His research interests include microscale gas breakdown and field and space-charge limited emission.



ADAM M. DARR (S'18) received the B.S. degree in nuclear engineering from Purdue University, West Lafayette, IN, USA, where he is currently pursuing the Ph.D. degree in nuclear engineering with the Bioelectronics and Electrophysics Laboratory. His research interests include micro- and nanoscale field, thermal, photo-, and space-charge limited emission, and electroporation.



ALLEN L. GARNER (S'02–M'07–SM'13) received the B.S. degree (High Hons.) in nuclear engineering from the University of Illinois at Urbana-Champaign in 1996, the M.S.E. degree in nuclear engineering from the University of Michigan, Ann Arbor, in 1997, the M.S. degree in electrical engineering from Old Dominion University, Norfolk, VA, USA, in 2003, and the Ph.D. degree in nuclear engineering from the University of Michigan in 2006.

He was an Active Duty Naval Officer from 1997 to 2003, serving onboard the USS Pasadena (SSN 752) and as an instructor for the Prospective Nuclear Engineering Officer Course with Submarine Training Facility, Norfolk, VA, USA. He is currently a Commander in the Navy Reserves assigned to NAVSEA Acquisition, Washington, DC, USA. From 2006 to 2012, he was an Electromagnetic Physicist with GE Global Research Center, Niskayuna, NY, USA. Since 2012, he has been an Assistant Professor with the School of Nuclear Engineering, Purdue University, West Lafayette, IN, USA. His research interests include biomedical applications of pulsed power and plasmas, high power microwaves, and multiphysics modeling.

Prof. Garner was a recipient of the University of Michigan Reagents' Fellowship, the National Defense Science and Engineering Graduate Fellowship, two Meritorious Service Medals, the Navy and Marine Corps Commendation Medal, and five Navy and Marine Corps Achievement Medals. He is a Licensed Professional Engineer in Michigan.